

Journal of Materials Chemistry B

Accepted Manuscript



This is an *Accepted Manuscript*, which has been through the Royal Society of Chemistry peer review process and has been accepted for publication.

Accepted Manuscripts are published online shortly after acceptance, before technical editing, formatting and proof reading. Using this free service, authors can make their results available to the community, in citable form, before we publish the edited article. We will replace this *Accepted Manuscript* with the edited and formatted *Advance Article* as soon as it is available.

You can find more information about *Accepted Manuscripts* in the [Information for Authors](#).

Please note that technical editing may introduce minor changes to the text and/or graphics, which may alter content. The journal's standard [Terms & Conditions](#) and the [Ethical guidelines](#) still apply. In no event shall the Royal Society of Chemistry be held responsible for any errors or omissions in this *Accepted Manuscript* or any consequences arising from the use of any information it contains.

Cite this: DOI: 10.1039/c0xx00000x

COMMUNICATION

Highly luminescent and photostable near-infrared fluorescent polymer dots for long-term tumor cell tracking *in vivo*†

Liqin Xiong,^{*ab} Yixiao Guo,^b Yimin Zhang,^b Fengwen Cao^b

Received (in XXX, XXX) Xth XXXXXXXXX 20XX, Accepted Xth XXXXXXXXX 20XX

DOI: 10.1039/b000000x

Near-infrared-emitting polymer dots were prepared by encapsulating the dye NIR775 into the matrix of MEH-PPV dots using a nanoscale precipitation method, and their application for long-term tumor cell tracking *in vivo* is demonstrated for the first time.

In recent years, conjugated polymer dots have attracted increasing attention in the biomedical field because of their attractive chemical and optical features, such as bright fluorescence intensity, excellent photostability, high emission rates, and minimal cytotoxicity.¹⁻¹⁶ Of particular importance is the development of the near-infrared (NIR) emitting polymer dots where autofluorescence background is significantly decreased of *in vivo* fluorescence imaging.¹⁷⁻²⁰ Recently, Chiu lab has developed deep-red emission polymer dots for *ex vivo* imaging.²¹ Rao lab designed self-luminescing NIR polymer dots by integrating bioluminescence resonance energy transfer (BRET) and fluorescence resonance energy transfer (FRET) in an energy transfer relay for *in vivo* lymph node mapping and tumor targeting.²² Liu lab developed far-red/near-infrared (FR/NIR)-emissive conjugated polymer dots for *in vivo* tumor imaging.^{23,24} Very recently, we reported that the NIR775 dye-doped MEH-PPV polymer dots exhibited long-term colloidal stability and photostability in water at 4 °C for at least nine months, and were successfully applied to imaging vasculature of U87MG tumors in living mice after intravenous injection.²⁵ To date, only a few studies about the NIR-emitting polymer dots for *in vivo* cell tracking are reported.²⁴ Herein, we further use the NIR775 dye-doped MEH-PPV polymer dots system as fluorescent nanoprobe for the *in vitro* HeLa cell labeling and *in vivo* long-term HeLa tumor tracking.

Fluorescent cell labeling is as sensitive as radiolabel based imaging techniques, but without any exposure to irradiation. Fluorescent labeling provides an effective means of non-invasively tracking cells repeatedly, thereby providing insight into cell migration to the target site. In general, there are direct and indirect ways of labeling cells with nanoprobe. Direct labeling is comparatively easy, less expensive and a well-established methodology where the cells are labeled with nanoprobe and detected by relevant imaging modalities. Moreover, as each cell contains many nanoprobe that will be passed down to daughter cells, long-term monitoring of the cell's fate is feasible.²⁶⁻³⁰ Therefore, we chose direct fluorescent labeling of cells, in which the cells are incubated with the NIR

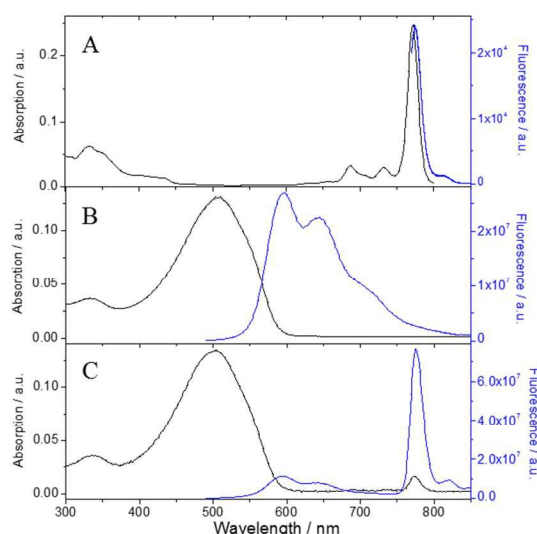


Fig. 1 Absorption and fluorescence spectra of the free NIR775 dyes (A), the free polymer dots (B), and the NIR polymer dots (C).

polymer dots in serum free media.

The NIR polymer dots were prepared according to our previous work by encapsulating the NIR dye, silicon 2,3-naphthalocyanine bis(trihexylsilyloxy) (NIR775), into the matrix of polymer dots, poly[2-methoxy-5-(2-ethylhexyloxy)-1,4-phenylenevinylene] (MEH-PPV).^{15,17} The NIR emission is realized based on a FRET system utilizing NIR775 dye as an acceptor and MEH-PPV polymer as a donor (Scheme S1). To minimize the self-quenching effect among encapsulated NIR775 and simultaneously get the highest FRET efficiency, the optimal ration of NIR775 to the MEH-PPV matrix (by weight) was found to be 0.012:1. The synthesized NIR polymer dots were 30–50 nm in diameter (Fig. S1). This result is consistent with previous studies.²²

Fig. 1 shows the absorption and emission spectra of the free NIR775 dyes, undoped MEH-PPV, and NIR775-doped MEH-PPV polymer dots (NIR polymer dots). The free NIR775 dyes dissolved in THF exhibit an absorption peak at 772 nm and strong fluorescence emission at 774 nm. The undoped MEH-PPV polymer dots show a broad absorption band with a maximum at 504 nm and intense emission at 598 nm with a shoulder at 643

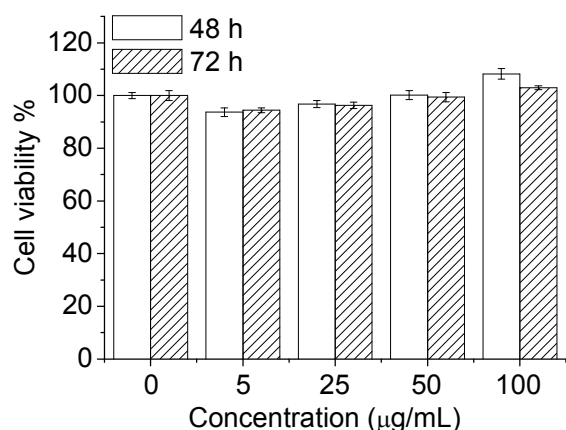


Fig. 2 Viability values (%) of cells estimated by CCK-8 assay versus incubation concentrations of the NIR polymer dots. Data represent mean \pm SD (n = 6).

nm. The dominant absorption peaks (around 504 nm) of the NIR polymer dots are due to MEH-PPV, whereas relatively weak absorption (around 772 nm) from the dopant NIR775 can also be observed. With 468 nm excitation, the fluorescence from MEH-PPV is almost completely quenched, and the NIR polymer dots exhibit strong fluorescence peak from the dopant molecule at 776 nm, indicating efficient FRET from the MEH-PPV to NIR775.

The absorbance and fluorescence spectra of NIR775 doped in MEH-PPV dots were similar to the spectra of free NIR775 dyes. However, their excitation spectra are different. The most intense peak of NIR775 doped in MEH-PPV dots is centered at 468 nm, while the excitation peak of the free NIR775 is 764.5 nm (Fig. S2). And we compared fluorescence intensity of NIR775 doped in MEH-PPV dots under 468 nm and 764.5 nm excitation, respectively (Fig. S3). When excited at 468 nm in aqueous solution, the NIR fluorescence intensity is 10 times stronger than that under excitation at 764.5 nm, confirming efficient FRET occurred from the MEH-PPV matrix to the NIR775 in the synthesized NIR polymer dots.

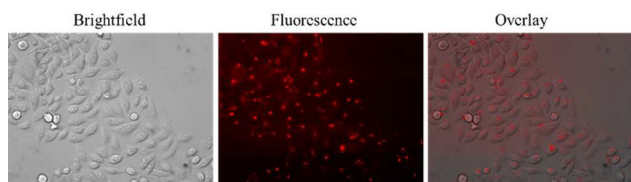


Fig. 3 Fluorescence imaging of HeLa cells incubated with NIR polymer nanoparticles (\sim 5 μ g) for 30 h. excitation: 480/30 nm, dichroic beamsplitter: Q570LP, emission: D755/40M; acquisition time: 1 s.

The cytotoxicity of the NIR polymer dots was evaluated by the CCK-8 assay in HeLa cells (Fig. 2). The viability of H1299 cells above a 5–100 μ g/mL concentration of NIR polymer dots was slightly increased. After 48 h of incubation with polymer dots at a concentration of 100 μ g/mL, the cellular viabilities were estimated to be greater than 108%. Even after 72 h of incubation with polymer dots at a concentration of 100 μ g/mL, cells maintained greater than 102% cell viability. These results demonstrated the weak toxic effects of NIR polymer dots on cell viability in these conditions.

We chose direct cell labeling techniques for cellular tracking, in which HeLa cells in the culture plate were incubated with 5 μ g/mL NIR polymer dots at 37°C overnight, and the cells were washed three times with culture medium before cell imaging. Approximately 100% of HeLa cells were labeled with dots under the fluorescence microscope (Fig. 3). And the endocytosed NIR polymer dots within HeLa cells was distributed mainly in the cytoplasm.

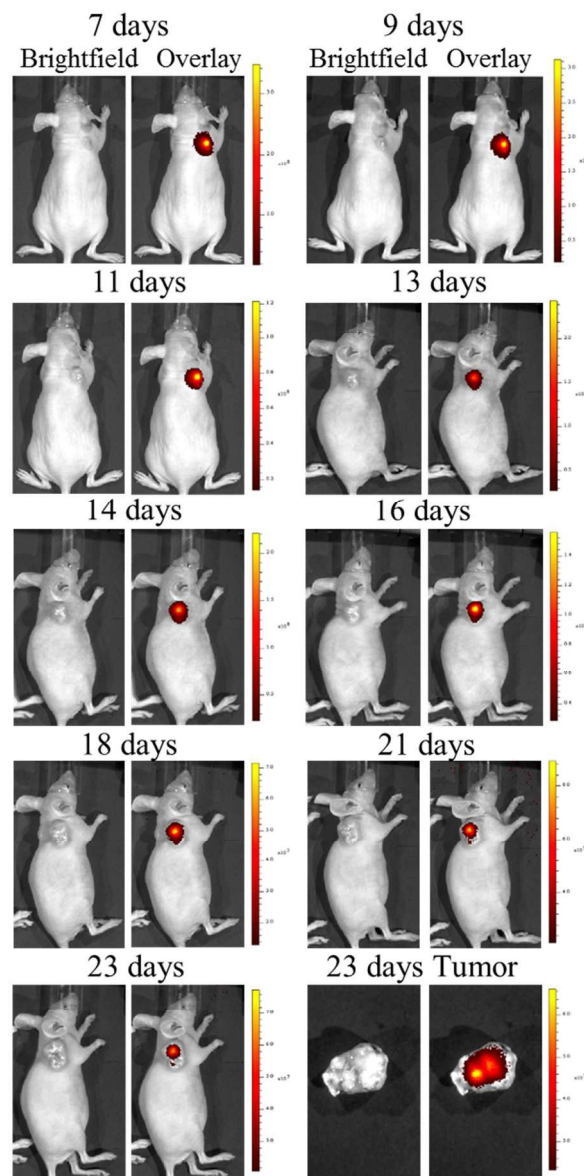


Fig. 4 Time-dependent *in vivo* fluorescence (FL) and brightfield (BF) imaging of the mouse injected with the NIR polymer nanoparticles (\sim 20 μ g) incubated HeLa cells and *ex vivo* fluorescence imaging of the tumor excreted from the mouse after 23 days injection. (Excitation filter: 465 \pm 15 nm; emission filter: 780 \pm 10 nm).

To investigate the long-term labeling capability and toxicity of the NIR polymer dots, 2×10^5 HeLa cells treated with 20 μ g of NIR polymer dots were subcutaneously injected into a nude mouse. The mouse was imaged at different time after injection using the IVIS spectrum imaging system (Fig. 4). The NIR

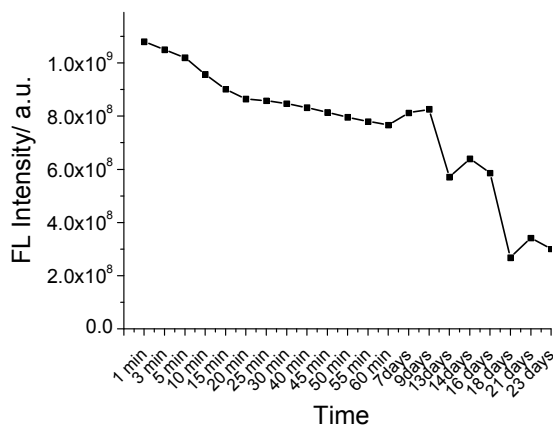


Fig. 5 Region of interest (ROI) analysis of the fluorescence intensity of the NIR polymer nanoparticles ($\sim 20 \mu\text{g}$) incubated HeLa cells in the mouse over time.

polymer dots remains 75% of its fluorescence upon 7 days injection and still retains 28% of fluorescence after 23 days (Fig. 5, Fig. S4), indicating the durable brightness and long-term photostability of the NIR polymer dots. Moreover, *ex vivo* imaging of tumors showed that strong NIR fluorescence signal was detected in almost the whole region of the tumor, suggesting that the NIR polymer dots could be inherited by daughter cells. In addition, after 7 days injection, the size of the grafted tumor reached $\sim 0.2 \text{ cm}$, which is recognized to the naked eyes, and tumor kept growing up to $\sim 1.5 \text{ cm}$ after 23 days, indicated that the NIR polymer dots had no obvious effect on the tumor growth. These data indicated that $20 \mu\text{g}$ could be considered a safe labeling dosage of the NIR polymer dots with no detectable influence on tumor formation ability over 23 days.

We examined the difference in sensitivity by using lower concentration ($5 \mu\text{g}$, $10 \mu\text{g}$) of the NIR polymer dots. Significant fluorescence signals was detected up to 20 days for $10 \mu\text{g}$ of dots-treated cells and 15 days for $5 \mu\text{g}$ of dots-treated cells (Fig. 6). Furthermore, *ex vivo* imaging of tumors showed that intense

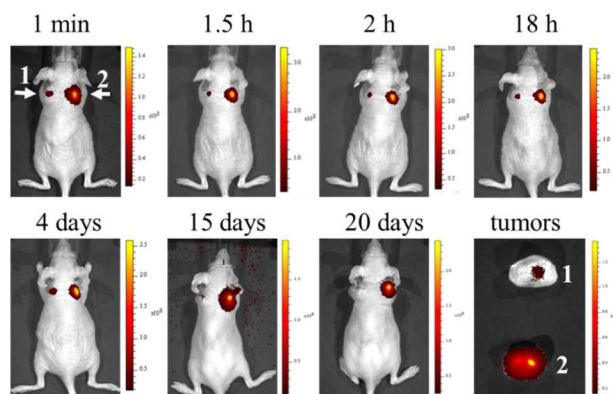


Fig. 6 Time-dependent *in vivo* fluorescence of the mouse injected with different concentration of the NIR polymer nanoparticles (I: $\sim 5 \mu\text{g}$, 2: $\sim 10 \mu\text{g}$) incubated HeLa cells and *ex vivo* fluorescence imaging of the tumors excised from the mouse after 20 days injection.

fluorescence signal was observed in the tumor formed by $5 \mu\text{g}$ of dots-treated cells, indicating the high sensitivity of the NIR polymer dots for long-term cell tracking. Tumor tissues from $5 \mu\text{g}$ of dots-treated cells were excised for sectioning and imaging under a fluorescence microscope. Strong near-infrared fluorescence was observed within the tumor tissue, confirmed the NIR polymer dots in the tumors (Fig. S5).

We further test the difference in sensitivity between fluorescence and bioluminescence of NIR polymer dots by conjugated with Luc8 by EDC-mediated coupling reaction according to Rao lab's work.²² The FRET efficiency of the NIR polymer dots was calculated to be about 0.77, and the overall BRET ratio of the Luc8-conjugated NIR polymer dots, determined by dividing the acceptor emission ($551\text{--}810\text{nm}$) by the donor emission ($400\text{--}550\text{nm}$), was about 2.5 (corresponding to an efficiency of 0.71). The prepared Luc8-conjugated NIR polymer dots with different concentration ($3 \mu\text{g}$, $0.6 \mu\text{g}$, $0.3 \mu\text{g}$, $0.06 \mu\text{g}$) were subcutaneously injected into a nude mouse. The mouse was imaged immediately after an intravenous injection of $10 \mu\text{g}$ of coelenterazine for bioluminescence imaging with 1 minute acquisition time for no emission filter and 3 minutes acquisition time for NIR emission filter ($780 \pm 10 \text{ nm}$). Following bioluminescence imaging, *in vivo* fluorescence imaging was carried out with 2 second acquisition time (excitation: $465 \pm 15 \text{ nm}$; emission: $780 \pm 10 \text{ nm}$) (Fig. 7 and Table S1). Intense NIR fluorescence signals were clearly visualized in the four injection sites, while bioluminescence imaging showed no obvious signal in the injection IV, indicating the high luminescence intensity and sensitivity of NIR polymer dots as a probe for fluorescence imaging. Although bioluminescence imaging showed high signal to background ratio with the value was 349.3, 20.2, 11.6, and 6.2 for $3 \mu\text{g}$, $0.6 \mu\text{g}$, $0.3 \mu\text{g}$, and $0.06 \mu\text{g}$ of Luc8-conjugated dots (without emission filter), respectively. After using the NIR emission filter ($780 \pm 10 \text{ nm}$), the signal to background ratio was decreased to 12.3, 5.6, 3.8, and 1.8, respectively. Fluorescence imaging using NIR polymer dots as a probe compared to NIR bioluminescence imaging showed a similar signal to background ratio with the value was 3.7, 2.9, 1.5, and 1.0, respectively, and decreased the exposure time by >90 -fold, which benefitted the monitoring of quick interactions of cells.

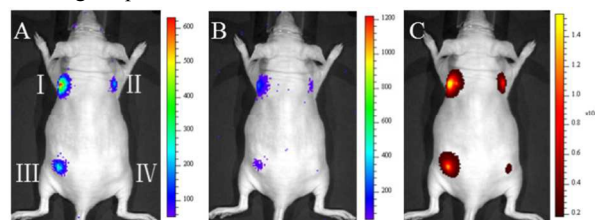


Fig. 7 *In vivo* bioluminescence (A, B) and fluorescence (C) imaging of the mouse injected with different concentration of the Luc8-conjugated NIR polymer nanoparticles subcutaneously (I: $3 \mu\text{g}$, II: $0.3 \mu\text{g}$, III: $0.6 \mu\text{g}$, IV: $0.06 \mu\text{g}$). A, open without filter, acquisition time: 1 min; B, with $780 \pm 10 \text{ nm}$ filter, acquisition time: 3 min; C, Excitation filter: $465 \pm 15 \text{ nm}$; emission filter: $780 \pm 10 \text{ nm}$, acquisition time: 2 s.

The ability to monitor cell survival, migration and differentiation is essential for the success of cell based therapies. Certain sized nanoparticles allow efficient particle-cell interaction, which permit non-invasive, accurate and real-time cell tracking.

However, it is still big challenge to understanding the fate of cells *in vivo* by fluorescence imaging or magnetic resonance imaging.^{26,30-32} In this study, 2×10^5 HeLa cells incubated with different concentration (5 μg , 10 μg , 20 μg) of NIR polymer dots were subcutaneously injected into a nude mouse. Strong fluorescence signals was detected up to 25 days (Fig. S6). The NIR polymer dots still remains 34% (site 1), 23% (site 2), and 33% (site 3) of its fluorescence after 25 days, respectively (Fig. S7). At 25 days after injection, the mouse was scarified and surgically opened for imaging. All the three injection sites were detected the NIR fluorescence signals. However, brightfield image of the mouse showed that only two tumors were detected in the site 1 and 2, respectively. These data indicated that the fate of cells *in vivo* is unknown by the direct fluorescent cell labelling method. Although bioluminescence imaging was reported to be able to tracking the fate and function of cell *in vivo*, it is not applicable clinically.³³ On the other hand, *ex vivo* imaging of tumors showed that strong fluorescence signal were observed in the tumors formed by 5 μg and 10 μg of dots-treated cells, highlighting the long-term labeling capability of the polymer dots as a probe for NIR fluorescence imaging.

In conclusion, we prepared the NIR-emitting polymer dots by encapsulating the dye NIR775 into the matrix of MEH-PPV dots using a nanoprecipitation method, and demonstrated the synthesized NIR polymer dots for long-term tumor cell tracking *in vivo* for the first time. These synthesized NIR polymer dots showed no obvious effect on the tumor growth, and exhibited unique capabilities for *in vivo* cell tracking, such as long-term luminescence and photostability, and high sensitivity. This study provides a foundation for the development of the whole-body tumor cell tracking based on the NIR polymer dots as fluorescent nanoprobles.

This work was supported by grants from the Natural Science Foundation Project of China (no. 81301261, no. 21374059), the Shanghai Pujiang Project (no. 13PJ1405000), and Doctoral Fund of Ministry of Education of China (no. 20130073120098). We gratefully acknowledge Prof. Jianghong Rao for providing advice on the project, and we acknowledge the use of the SCI³ Core Facility.

Notes and references

^a Department of Nuclear Medicine, Rui Jin Hospital, School of Medicine, Shanghai Jiao Tong University, Shanghai, 200025, P. R. China. *E-mail: xiongliqin@sjtu.edu.cn

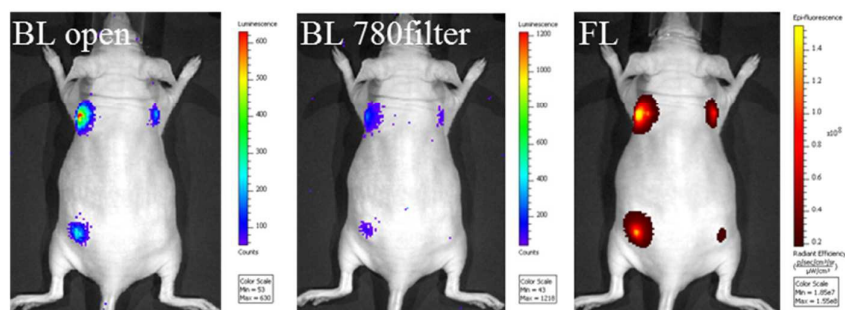
^b School of Biomedical Engineering, Med-X Research Institute, Shanghai Jiao Tong University, Shanghai, 200030, P. R. China.

† Electronic Supplementary Information (ESI) available: [details of the experiment section, TEM, Excitation spectra, Fluorescence spectra, fluorescence images of mice, ROI analysis of the fluorescence intensity].

See DOI: 10.1039/b000000x/

- J. Pecher and S. Mecking, *Chem. Rev.*, 2010, **110**, 6260-6279.
- C. F. Wu and D. T. Chiu, *Angew. Chem. Int. Ed.*, 2013, **52**, 3086-3109.
- C. L. Zhu, L. B. Liu, Q. Yang, F. T. Lv and S. Wang, *Chem. Rev.*, 2012, **112**, 4687-4735.
- K. Li and B. Liu, *Chem. Soc. Rev.*, 2014, **43**, 6570-6597.
- L. Wei, P. Zhou, Q. X. Yang, Q. Y. Yang, M. Ma, B. Chen and L. H. Xiao, *Nanoscale*, 2014, **6**, 11351-11358.
- C. F. Wu, B. Bull, C. Szymanski, K. Christensen and J. McNeill, *ACS Nano*, 2008, **2**, 2415-2423.

- G. X. Feng, K. Li, J. Liu, D. Ding and B. Liu, *Small*, 2014, **10**, 1212-1219.
- S. Kim, C. K. Lim, J. Na, Y. D. Lee, K. Kim, K. Choi, J. F. Leary and I. C. Kwon, *Chem. Commun.*, 2010, **46**, 1617-1619
- Y. Zhang, J. Yu, M. E. Gallina, W. Sun, Y. Rong and D. T. Chiu, *Chem. Commun.*, 2013, **49**, 8256-8258.
- C. F. Wu, T. Schneider, M. Zeigler, J. B. Yu, P. G. Schiro, D. R. Burnham, J. D. McNeill and D. T. Chiu, *J. Am. Chem. Soc.*, 2010, **132**, 15410-15417.
- Y. Wan, L. Zheng, Y. Sun and D. Zhang, *J. Mater. Chem. B*, 2014, **2**, 4818-4825.
- G. Feng, J. Liu, J. Genga and B. Liu, *J. Mater. Chem. B*, 2015, **3**, 1135-1141.
- Y. H. Jin, F. M. Ye, M. Zeigler, C. F. Wu and D. T. Chiu, *ACS Nano*, 2011, **5**, 1468-1475.
- A. Wagh, S. Y. Qian and B. Law, *Bioconjugate Chem.*, 2012, **23**, 981-992.
- I.-C. Wu, J. Yu, F. Ye, Y. Rong, M. E. Gallina, B. S. Fujimoto, Y. Zhang, Y.-H. Chan, W. Sun, X.-H. Zhou, C. Wu, and D. T. Chiu, *Am. Chem. Soc.*, 2015, **137**, 173-178.
- J. Geng, C. Sun, J. Liu, L.-D. Liao, Y. Yuan, N. Thakor, J. Wang, and B. Liu, *Small*, 2015, **11**, 1603-1610.
- X. Wu, X. Sun, Z. Guo, J. Tang, Y. Shen, T. D. James, H. Tian, and W. Zhu, *J. Am. Chem. Soc.*, 2014, **136**, 3579-3588.
- Z. Guo, S. Park, J. Yoon and I. Shin, *Chem. Soc. Rev.*, 2014, **43**, 16-29.
- L. Q. Xiong, T. S. Yang, Y. Yang, C. J. Xu and F. Y. Li, *Biomaterials*, 2010, **31**, 7078-7085.
- L. Q. Xiong, Z. G. Chen, Q. W. Tian, T. Y. Cao, C. J. Xu and F. Y. Li, *Anal. Chem.*, 2009, **81**, 8687-8694.
- C. F. Wu, S. J. Hansen, Q. Hou, J. B. Yu, M. Zeigler, Y. H. Jin, D. R. Burnham, J. D. McNeill, J. M. Olson and D. T. Chiu, *Angew. Chem. Int. Ed.*, 2011, **50**, 3430-3434.
- L. Q. Xiong, A. J. Shuhendler and J. H. Rao, *Nat. Commun.*, 2012, **3**:1193.
- K. Li, D. Ding, D. Huo, K. Pu, N. N. P. Thao, Y. Hu, Z. Li and B. Liu, *Adv. Funct. Mater.*, 2012, **22**, 3107-3115.
- J. Liu, K. Li, and B. Liu, *Adv. Sci.*, 2015, **2**, 1500008.
- L. Q. Xiong, F. Cao, X. Cao, Y. Guo, Y. Zhang and X. Cai, *Bioconjug Chem.*, 2015, **26**, 817-821.
- K. Y. Pu, A. J. Shuhendler, M. P. Valta, L. Cui, M. Saar, D. M. Peehl and J. H. Rao, *Adv. Healthc. Mater.*, 2014, **3**, 1292-1298.
- G. Chen, F. Tian, Y. Zhang, Y. Zhang, C. Li and Q. Wang, *Adv. Funct. Mater.*, 2014, **24**, 2481-2488.
- N. M. Idris, Z. Li, L. Ye, E. K. W. Sim, R. Mahendran, P. C. L. Ho and Y. Zhang, *Biomaterials*, 2009, **30**, 5104-5113.
- W. J. Parak, T. Pellegrino and C. Plank, *Nanotechnology*, 2005, **16**, R9-R25.
- A. Bhirde, J. Xie, M. Swierczewska and X. Chen, *Nanoscale*, 2011, **3**, 142-153.
- P. Jendelová, V. Herynek, J. DeCroos, K. Glogarová, B. Andersson, M. Hájek and E. Syková, *Magn. Reson. Med.*, 2003, **50**, 767-776.
- N. Ma, H. Cheng, M. Lu, Q. Liu, X. Chen, G. Yin, H. Zhu, L. Zhang, X. Meng, Y. Tang and S. Zhao, *Sci Rep.*, 2015, **5**, 9058.
- P. E. de Almeida, J. R. M. van Rappard and J. C. Wu, *Am J Physiol Heart Circ Physiol*, 2011, **301**, H663-H671.



Near-infrared-emitting polymer dots were prepared by encapsulating the dye NIR775 into the matrix of MEH-PPV dots using a nanoscale precipitation method, and their application for long-term tumor cell tracking in vivo is demonstrated. These synthesized NIR polymer dots showed no obvious effect on the tumor growth, and exhibited unique capabilities for in vivo cell tracking, such as long-term luminescence and photostability, and high sensitivity.